DOI: 10.1002/ejoc.200500903

Synthesis and Photophysical Properties of a Pyrazolino[60]fullerene with Dimethylaniline Connected by an Acetylene Linkage

Andreas Gouloumis,[a] Frédéric Oswald,[a] Mohamed E. El-Khouly,[b,c] Fernando Langa,*[a] Yasuyuki Araki,[b] and Osamu Ito*[b]

Keywords: Fullerenes / Electron transfer / Microwave irradiation / Photophysical properties

A new triad based on pyrazolino[60]fullerene and a conjugated dimethylaniline group has been synthesized by a copper-free Sonogashira cross-coupling reaction using microwave irradiation as the source of energy. The electrochemical and photophysical properties of the triad were systematically investigated by techniques such as time-resolved fluorescence and transient absorption spectroscopy. Charge separation via the excited singlet state of the C_{60} moiety was confirmed in polar and nonpolar solvents and competes with triplet formation of the C_{60} moiety. The charge-separated state persisted for 91 ns. Such long lifetimes are characteristic of long distances between the radical anion of the pyrazolino[60]fullerene derivative and the radical cation of the dimethylaniline moiety.

Introduction

Fullerenes are characterized by remarkably strong electron-accepting properties, similar to those of quinones.[1] These characteristics, together with their electronic absorption properties,[2] make them promising chromophores in photodriven redox processes and, as a consequence, they have potential applications in molecular and supramolecular electronics, light harvesting and photocatalysis.[3] The synthesis of C_{60}-based systems that incorporate an electron-donor fragment continues to attract considerable interest in an effort to obtain efficient intramolecular electron transfer and to generate long-lived charge-separated states in these donor–acceptor (D–A) molecular assemblies.[4] In this respect, various donor–spacer–fullerene systems, in which the donor is an amino group, have been prepared[5] and some of them show efficient charge separation.

In an effort to increase the lifetime of the charge-separated (CS) state in D–A arrays, two strategies have been used: (i) The separation between the donor (D) and the acceptor (A) has been increased and (ii) a reduction gradient between D and A[6] has been introduced by insertion of additional electroactive moieties.[7] In the final CS state, the charges are well-separated and this slows the back-electron-transfer process and increases the lifetime of the CS state.

In recent years we have focused our attention on studying the synthesis and properties of pyrazolino[60]fullerene derivatives,[8] which can be prepared by 1,3-dipolar cycloaddition of nitrile imines to C_{60}.[9] Nitrile imines can be prepared in situ from hydrazones, meaning that the overall reaction can be performed in one pot with good yields.[10] Photophysical studies of pyrazolino[60]fullerene derivatives have revealed efficient electron transfer from the electron pair of the pyrazoline sp^3 nitrogen atom to the C_{60} cage.[11]

In an attempt to enhance intramolecular electron transfer by utilizing a reduction gradient (through the sp^3 nitrogen atom of the pyrazoline ring) in order to increase the separation between the donor and the acceptor we report here a novel donor–C_{60} triad **1** that incorporates a pyrazolino[60]fullerene (C_{60}Pz) as the acceptor and a dimethylaminophenylethynylphenyl moiety connected to the N1 atom of the pyrazoline ring as the donor (Scheme 1). Theoretical calculations have been performed along with electrochemical and photochemical studies.

Results and Discussion

Synthesis

Pyrazolino[60]fullerene **1** was synthesized by two methods (Scheme 1) starting from hydrazone **2**, which was obtained in 75% yield by reaction of the corresponding benzaldehyde and 4-iodophenylhydrazine according to a standard procedure.[8] By route (a), a solution of hydrazone **2** in benzene was treated with NCS at 0 °C under argon. A solution of C_{60} in toluene and Et_3N were then added and

---

[a] Facultad de Ciencias del Medio Ambiente, Universidad de Castilla-La Mancha,
45071 Toledo, Spain
E-mail: Fernando.LPuente@uclm.es
[b] Institute of Multidisciplinary Research for Advanced Materials, Tohoku University,
Katahira, Sendai, 980-8577, Japan
E-mail: ito@tagen.tohoku.ac.jp
[c] Department of Chemistry, Graduate School of Education, Kafr El-Sheikh, Tanta University,
Tanta, Egypt

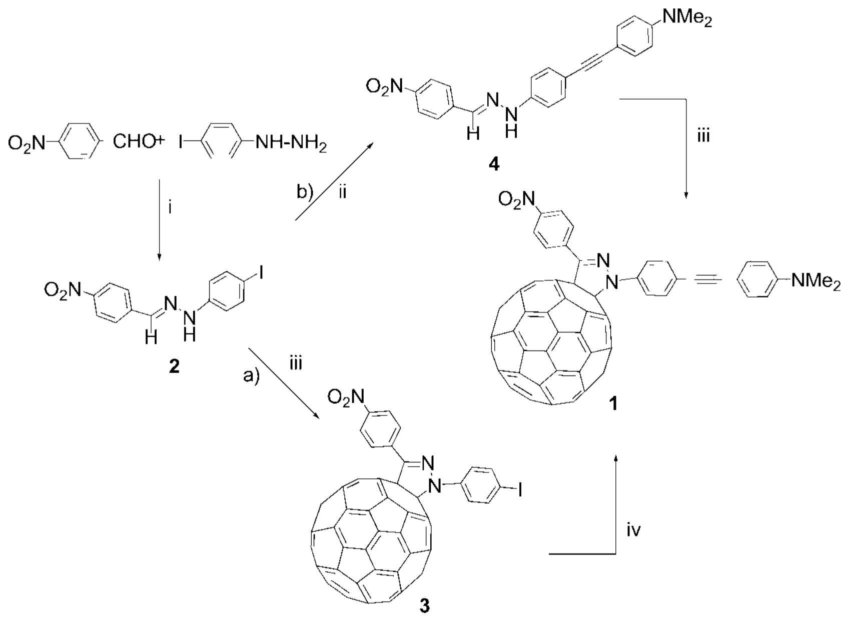

Scheme 1. Reagents and conditions: (i) AcOH, EtOH, 30 min, reflux; (ii) 4-(dimethylamino)phenylacetylene, CuI, PPh_3, piperidine, $[(PPh_3)_2PdCl_2]$, reflux, 4 h; (iii) 1) NCS, pyridine, 20 min then 2) C_{60}, toluene, Et_3N, microwaves, 50 min ; (iv) 4-(dimethylamino)phenylacetylene, piperidine, $[Pd(Ph_3)_4]$, chlorobenzene, microwaves, 40 min.

the mixture was irradiated for 50 min (210 W power) in a focused microwave reactor to afford **3** in 26% yield after purification by column chromatography (silica gel, toluene).

All attempts to perform the classical Pd/Cu-mediated cross-coupling (Sonogashira coupling)[12] reaction between **3** and 4-(dimethylamino)phenylacetylene using various solvents and bases failed in our hands. The failure of this procedure led us to turn to a second methodology based on a copper-free Sonogashira cross-coupling reaction.[13] Following this procedure, **3** and 4-(dimethylamino)phenylacetylene were allowed to react in chlorobenzene under microwave irradiation (300 W) in a single-mode apparatus (see Expt. Sect.) for 40 min in the presence of an excess of piperidine and 10 mol-% $[Pd(Ph_3)_4]$. This reaction led to the formation of **1** in moderate yield after flash column chromatography. Note that only one example of the Pd/Cu cross-coupling reaction with compounds containing fullerenes has been reported previously.[14]

In order to increase the yield of **1**, route (b) was attempted (Scheme 1), which is based on the Sonogashira cross-coupling of hydrazone **2** and 4-(dimethylamino)phenylacetylene and subsequent cycloaddition to C_{60}. Hydrazone **4** was prepared in 73% yield by the reaction of **2** with 4-(dimethylamino)phenylacetylene under palladium-catalyzed conditions[15] (see Scheme 1) for 4 h under reflux. The synthesis of cycloadduct **1** from hydrazone **4** was achieved by 1,3-dipolar cycloaddition of the intermediate nitrile imine to C_{60}, as described above for the synthesis of **3**. Subsequent purification by column chromatography (silica gel, toluene) gave **1** in 30% yield.

The structures of all compounds were fully supported by UV/Vis, FTIR and ^1H and ^{13}C NMR spectroscopy. The structures of both fullerene derivatives **1** and **3** were also confirmed by their MALDI-TOF mass spectra, which showed the expected molecular ions at m/z = 1101 and 1084, respectively.

Molecular Orbital Calculations

The most stable geometry of the targeted cycloadduct **1** was obtained by theoretical calculations at the AM1 level and the structure is shown in Figure 1. In a similar way to other pyrazolino[60]fullerene derivatives,[16] the *C*-substituent (the *p*-nitrophenyl group) is almost coplanar with respect to the pyrazoline ring (dihedral angle = 3.6°) and the *N*-substituent {the 4-[4-(dimethylamino)phenylethynyl]phenyl moiety} is twisted by 44°, indicating a lack of conjugation between the two moieties. The distance between the dimethylaniline (DMA) group and the edge of the C_{60}

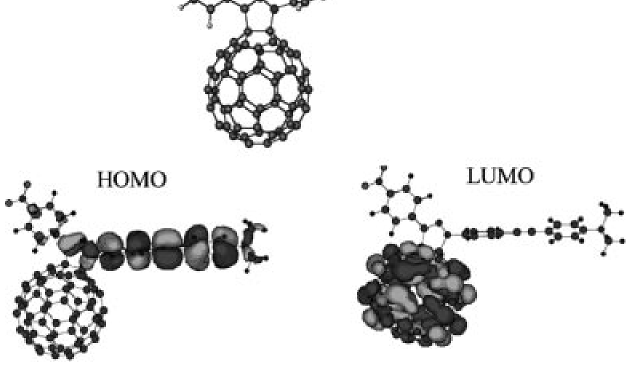

Figure 1. AM1-optimized structure of **1** (upper) and the HOMO and LUMO (lower).

(R_{D-A}) is 13.32 Å (22.11 Å with respect to the center), a distance that should allow a charge-separated state with a long life. Finally, the HOMO (E = –8.97 eV) and the LUMO (E = –3.05 eV) are centered on the 4-[4-(dimethylamino)phenylethynyl]phenyl moiety and the C_{60} cage, respectively (see Figure 1). Note that an appreciable amount of the electron density of the HOMO is present on the pyrazole moiety, which acts as an electron donor with respect to the C_{60} cage.

Electrochemical Measurements

The electrochemical behavior of C_{60}, triad **1** and model compounds **3** and **4** in benzonitrile was studied by cyclic voltammetry (CV) and Osteryoung square-wave voltammetry (OSWV). The results are summarized in Figure 2 and Table 1.

Table 1. Electrochemical data [V vs. Ag/AgNO$_3$] for the redox processes of compounds **1**, **3**, **4** and C_{60} fullerene detected by OSWV in benzonitrile solution (0.1 M n-Bu$_4$NClO$_4$) at room temperature under identical experimental conditions.[a]

	$E_{red}{}^{1[b]}$	$E_{red}{}^{2[b]}$	$E_{red}{}^{3[c]}$	$E_{red}{}^{4}$	$E_{red}{}^{5[b]}$	$E_{ox}{}^{1[c]}$
1	–0.88	–1.31	–1.56	–1.83[d]	–2.35	0.35
3	–0.88	–1.29	–1.52	–1.79[d]	–2.31	–
4	–	–	–1.50[e]	–1.78[e]		0.18[e]
C_{60}	–0.88	–1.31	–	–1.80	–2.28	–

[a] OSWVs were obtained using a sweep width of 25 mV, a frequency of 15 Hz, a step potential of 4 mV and a quiet time of 2 s on a Windows®-driven Autolab PGSTAT 30 electrochemical analyzer. [b] C_{60}-based reduction. [c] p-Nitrobenzene-based redox process. [d] The third C_{60}-based reduction wave was overlapped by the second p-nitrobenzene-based reduction wave. [e] Hydrazone-based reduction or oxidation.

The CV shows that triad **1** is electrochemically active in both anodic and cathodic sweep directions between +1.8 and –2.5 V. In the anodic scan, the redox process observed is chemically irreversible under the experimental conditions and is assigned to the dimethylaniline moiety (E_p = 0.35 V at 100 mV s^{-1}) by direct comparison with the processes for model compounds **3** and **4**. In model compound **4** this potential is observed at E_p = 0.18 V, meaning that an anodic displacement of about 0.17 V for this process can be observed in triad **1**.

In the cathodic scan, triad **1** exhibits five reduction waves (see Figure 2) which can be easily assigned by comparison with scans of the model compounds: The first and second waves are assigned to the C_{60} fullerene cage, the third to the p-nitrophenylpyrazoline moiety and the fourth process is due to the overlap of the third C_{60} fullerene potential and the second of the pyrazoline unit. The first three waves are electrochemically reversible ($\Delta E_p \approx$ 60 mV at 100 mV s^{-1}) and the fourth is quasi-reversible ($\Delta E_p \approx$ 100 mV at 100 mV s^{-1}).

The E_{red} and the first E_{ox} values enabled the free energies (ΔG_{CR}) of the radical ion pair to be calculated from the Weller relation [Equation (1)],[17] where ΔG_S refers to the static energy which is calculated using Equation (2) in benzonitrile and Equation (3) in toluene.[18]

$$-\Delta G_{CR} = E_{ox} - E_{red} - \Delta G_S \tag{1}$$

$$\Delta G_S = e^2/(4\pi\varepsilon_0\varepsilon_R R_{D-A}) \tag{2}$$

$$\Delta G_S = e^2/4\pi\varepsilon_o\{[1/(2R_+) + 1/(2R_-) - 1/R_{D-A}](1/\varepsilon_s) - [1/(2R_+) + 1/(2R_-)](1/\varepsilon_R)\} \tag{3}$$

The terms e, ε_0 and ε_R refer to elementary charge, vacuum permittivity and the static dielectric constant of the solvent used for rate and redox-potential measurements, respectively. The ΔG_{CR} and excited energy (E_{00}) values allowed the free-energy changes for the charge-separation process (ΔG_{CS}) to be calculated from Equation (4) (see Table 2).

$$-\Delta G_{CS} = E_{00} - (-\Delta G_{CR}) \tag{4}$$

The ΔG_{CS} values for **1** show that the charge-separation process via the excited singlet state of C_{60} ($^1C_{60}$*) is exothermic in both toluene and benzonitrile.

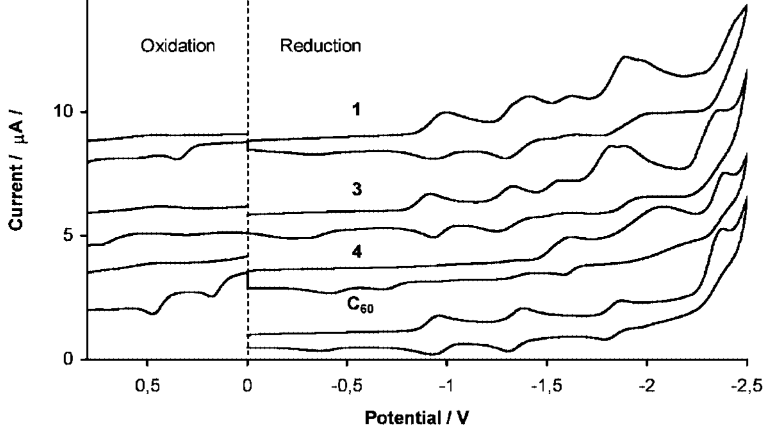

Figure 2. Cyclic voltammograms (sweep rate = 0.1 V s^{-1}) for **1**, **3**, **4** and C_{60} in benzonitrile containing n-Bu$_4$NClO$_4$ at room temperature.

Table 2. Free-energy changes (ΔG_{CS} and ΔG_{CR}), fluorescence lifetimes (τ_f) of $^1C_{60}*$, rate constants (k_{CS}) and quantum yield (Φ_{CS}) of charge separation, rate constants of charge recombination (k_{CR}) and radical-ion-pair lifetime of **1** in benzonitrile (BN) and toluene.

Solvent	ΔG_{CS} [eV]	τ_f [ps]	k_{CS} [10^9 s^{-1}]	Φ_{CS}	ΔG_{CR} [eV]	k_{CR} [10^7 s^{-1}]	τ_{RIP} [ns]
BN	–0.52[a]	–[b]	–	–[a]	–1.23[a]	1.34	75
Toluene	–0.15[c]	130 (70%) 1400 (30%)	6.9[d] (5.0)[e]	0.90[d] (0.63)[e]	–1.60[c]	1.10	91

[a] From Equations (1), (2) and (4). In Equation (2), R_{D-A} = 13 Å. [b] The fluorescence decay of C_{60} was overlapped by a broad fluorescence in the visible region. [c] From Equations (1), (3) and (4). In Equation (3), R_+ = 6.0 Å and R_- = 4.2 Å. [d] From Equations (5) and (6) employing the shorter fluorescence lifetime as τ_f for **1**; τ_{f0} = 1.3 ns for **3**. [e] On including the longer fluorescence lifetime as τ_f.

Steady-State Absorption Spectra

The absorption spectra of **1**, **3** and **4** were measured in benzonitrile and toluene in the range of 300–800 nm. Figure 3 (upper panel) shows the absorption spectrum of **3** which is characterized by an absorption band at 324 nm with a shoulder at 414 nm. The absorption spectrum of **4** is characterized by absorption peaks at 344 and 448 nm. The absorption spectra of **1** (Figure 3 lower panel) are a superimposition of the components, indicating that there is no significant ground-state electronic interaction. The strong absorption of the C_{60} moiety appears mainly in the UV region.

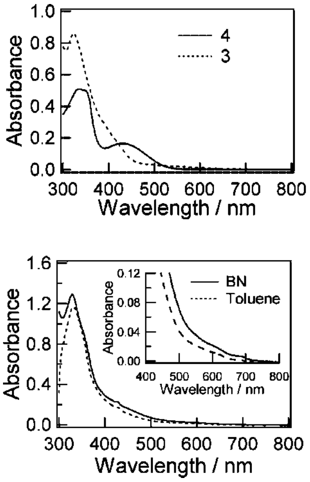

Figure 3. Steady-state absorption spectra of: **3** and **4** in toluene (upper panel) and triad **1** in toluene and benzonitrile (lower panel). The concentrations were kept at 0.02 mM.

Fluorescence Spectral Studies

The fluorescence spectrum of **1** in toluene upon applying 400 nm light as the excitation wavelength is shown in Figure 4. Two fluorescence peaks were observed at 450 and 700 nm; the latter peak can be attributed to the C_{60} moiety by comparison with the fluorescence of compound **3**. The intensity of the emission band of **1** monitored at 715 nm was significantly quenched compared to that of the C_{60} reference compound **3**. It was quite difficult to record the fluorescence of $^1C_{60}*$ in benzonitrile due to the weak emission at around 700 nm. These observations suggest efficient quenching of the singlet excited state of the C_{60} ($^1C_{60}*$) moiety by the appended donor entities. The 450 nm peak could be due to the emission of the donor moiety, although with a considerable red-shift from the fluorescence peak of **4**. Considerable quenching of the 450 nm fluorescence peak intensity was also observed, suggesting communication between the donor and C_{60} moieties.

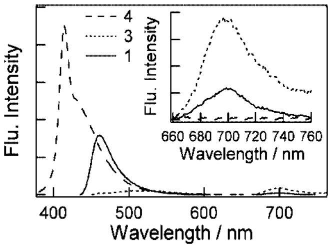

Figure 4. Steady-state fluorescence spectra of **1**, **3**, and **4** in toluene (concentrations are kept at 0.02 mM; λ_{ex} = 400 nm).

For **1** in benzonitrile, a broad fluorescence band was observed in addition to the 700 nm fluorescence peak of the C_{60} moiety.

Fluorescence Lifetime Measurements

The fluorescence time profiles of **1** in toluene are shown in Figure 5; the 700 nm fluorescence peak is observed to rise and the 450 nm fluorescence peak to decay, suggesting energy transfer from the excited singlet state of the donor moiety to the C_{60} moiety. From the initial decay rate of the 450 nm peak and the rise of the 700 nm peak, the rate of energy transfer can be evaluated to be 1.2×10^{10} s^{-1}.

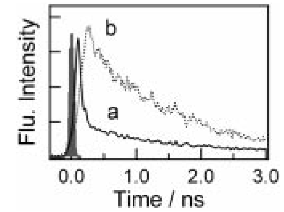

Figure 5. Fluorescence time profiles of **1** in toluene: (a) 450–600 nm and (b) 670–760 nm. (λ_{ex} = 400 nm; the shadow is the laser pulse profile).

The fluorescence time profile of C_{60} exhibited a single exponential decay with a lifetime (τ_{f0}) of 1.3 ns. The fluorescence decay time profile of **1** at 700 nm in toluene can be fitted with two exponential components: 130 ps (70%) and 1400 ps (30%). The shortening of the lifetime indicates that attaching donor moieties to C_{60} introduces a new quenching pathway for C_{60}. As a quenching process, it is most probable that charge separation from the donor moieties to the C_{60} moiety occurs, yielding a charge-separated (CS) state. The rate constants for charge separation (k_{CS}) were calculated from Equation (5),[19] where τ_{f0} and τ_f are the lifetimes of the reference and **1**, respectively. The quantum yields (Φ_{CS}) for the generation of the CS state via $^1C_{60}*$ were calculated from Equation (6).[19]

$$k_{CS} = (1/\tau_f) - (1/\tau_{f0}) \tag{5}$$

$$\Phi_{CS} = k_{CS}/(1/\tau_f) \tag{6}$$

The charge-separation rate constant (k_{CS}) and quantum yield (Φ_{CS}) were evaluated to be 6.9×10^9 s^{-1} and 0.90, respectively, in toluene from the shorter fluorescence lifetime, as listed in Table 2. By including the shorter fluorescence lifetime, they are reduced to 70%. In benzonitrile, the rate constant for the charge separation was not evaluated due to overlapping of the fluorescence band in the visible region.

Nanosecond Transient Spectra

The nanosecond transient absorption spectra of **1** and **3** were recorded in argon-saturated toluene and benzonitrile by applying 355 nm laser light excitation, which excites mainly the C_{60} moiety. In argon-saturated toluene, the transient spectra of **3** (Figure 6) exhibited mainly the characteristic band of the triplet state of the C_{60} moiety ($^3C_{60}*$) at 700 nm which has a decay rate of 4.0×10^5 s^{-1}.[20] The absence of radical ion pairs suggests no charge separation process. Similar observations were made in benzonitrile.

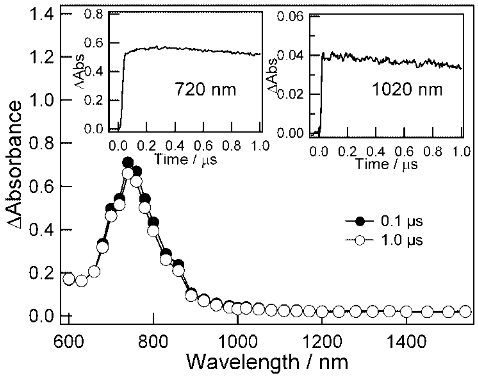

Figure 6. Transient absorption spectra obtained by 355 nm laser photolysis of **3** (0.1 mM) in argon-saturated toluene.

On the other hand, the transient absorption spectra of **1** (Figure 7) show a broad transient absorption band in the near-IR region with a rapid decay in addition to the $^3C_{60}*$ moiety at 700 nm with a slow decay. Although the characteristic peak of the radical anion of the C_{60} moiety ($C_{60}^{\cdot-}$) is expected to appear at 1000 nm, a broad band, which spreads widely across the range of 1000–1600 nm, may hide the $C_{60}^{\cdot-}$ peak at 1000 nm. We tentatively attributed this broad band to the radical cation of the donor moiety. Quite similar transient absorption spectra were observed in benzonitrile (Figure 7, upper panel) and toluene (Figure 7, lower panel), suggesting that similar photoinduced processes occur in polar and nonpolar solvents. Indeed, from the calculated ΔG_{CS} values, charge separation is possible in both benzonitrile and toluene.

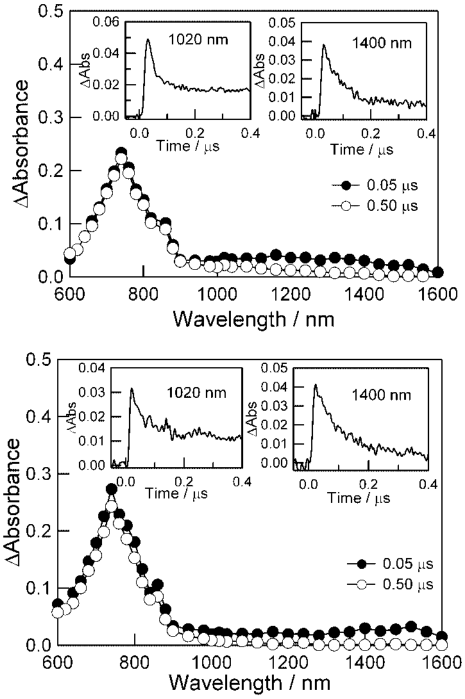

Figure 7. Transient absorption spectra obtained by 355 nm laser photolysis of **1** (0.1 mM) in argon-saturated benzonitrile (upper panel) and toluene (lower panel).

The broad band of the radical cation of the donor moiety was confirmed by measuring the nanosecond transient spectra of a mixture of C_{60} and **4** in benzonitrile by 355 nm laser light excitation (Figure 8). The transient absorption spectra exhibited growth of the absorption bands of $C_{60}^{\cdot-}$ at 1080 nm accompanied by a concurrent decay of the absorption band of $^3C_{60}*$ at 760 nm. Furthermore, a slow rise in absorption was clearly observed in the range 1100–1600 nm, which was attributed to the radical cation of **4** ($4^{\cdot+}$). The assignment of the broad absorption band to $4^{\cdot+}$ may be reasonable because the radical cation is widely delocalized from the dimethylaniline to the pyrazole ring via the phenylacetylene bridge, as shown in the representation of the HOMO of **1** in Figure 1. The rate constant for the bimolecular quenching of $^3C_{60}*$ (k_q) was evaluated to be 4.1×10^9 M^{-1}s^{-1}. The efficiency of the intermolecular electron transfer (Φ_{et}) was evaluated to be 0.60 from the ratio of the maximal concentration of the generated $C_{60}^{\cdot-}$ to the initial concentration of $^3C_{60}*$, with the maximal absorbance of $C_{60}^{\cdot-}$ being evaluated after subtracting the overlapping absorbance of $4^{\cdot+}$. The molar extinction coefficient of $4^{\cdot+}$ was evaluated to be 18000 M^{-1}cm^{-1} at 1250 nm employing the molar extinction coefficient of $C_{60}^{\cdot-}$ (14000 M^{-1}cm^{-1} at 1080 nm).[20]

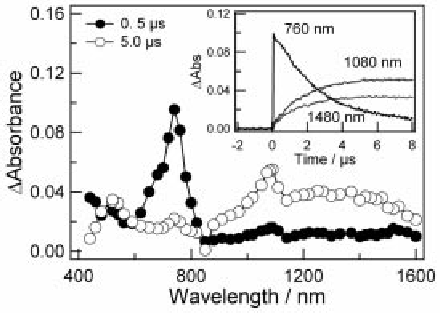

Figure 8. Transient absorption spectra obtained by 355 nm laser photolysis of C_{60} (0.1 mM) in the presence of **4** (1 mM) in argon-saturated benzonitrile.

From the time profiles measured at 1400 nm, the rate constants for the charge-recombination process (k_{CR}) of **1** were evaluated to be 1.34×10^7 (benzonitrile) and $1.10 \times 10^7\ s^{-1}$ (toluene). From k_{CR}, the lifetimes of the radical ion pairs (τ_{RIP}) were evaluated to be around 75 (benzonitrile) and 91 ns (toluene), which are quite long compared with the lifetimes of the charge-separated state reported for the dyads of C_{60} with dimethylaniline connected to a pyrrolidine ring.[5c,5d] The slightly shorter τ_{RIP} value in benzonitrile compared with toluene suggests that the charge-recombination process belongs to the inverted region of the Marcus parabola[21] since the reorganization energy may be less than the absolute value of the free-energy change of the charge-recombination process (ΔG_{CR}) even in benzonitrile.[22]

Energy Diagram

The energy diagram for the photophysical events after photoexcitation is based on the lowest excited-state data and calculated energy levels of R~$C_{60}^{\bullet -}$~C≡C–$DMA^{\bullet +}$ (Figure 9). The excited singlet state of the C_{60} moiety was evaluated from the fluorescence peak, whereas the excited triplet state was cited from the literature.[1,2,19c] The energy levels of R~$C_{60}^{\bullet -}$~C≡C–$DMA^{\bullet +}$ in polar solvents with similar dielectric constants determined from electrochemistry and photophysical measurements are reliable, although the energy level of R~$C_{60}^{\bullet -}$~C≡C–$DMA^{\bullet +}$ in toluene may be associated with considerable error. Our observations, however, revealed that the charge-separation process via the $^1C_{60}$* moiety is possible in polar and nonpolar solvents, whereas charge separation via the $^3C_{60}$* moiety could be impossible. Since the 355 nm light employed in the transient absorption measurements directly excites the C_{60} moiety, charge separation takes place via the $^1C_{60}$*moiety. In toluene, even if the donor moiety of **1** was excited, the excited energy transfers to the C_{60} moiety, from which the charge separation takes place. From the transient absorption spectra of **1** in Figure 7, the relative concentration of the radical cation of the donor moiety to the $^3C_{60}$* moiety can be evaluated to be 0.1, which implies that most of the radical ion pair disappeared immediately after the nanosecond laser pulse (6 ns) irradiation because the quantum yield of the charge separation was larger than 0.6.

Conclusion

A pyrazolino[60]fullerene with a dimethylaniline connected by an acetylene linkage has been synthesized for the first time and its electrochemical and photophysical properties have been systematically investigated by techniques including time-resolved fluorescence and transient absorption spectroscopy. The $^1C_{60}$* decays by intersystem crossing to populate the $^3C_{60}$* state and by charge separation to yield the radical ion pair in polar and nonpolar solvents. The former process seems to be dominant compared with the latter. The charge-separated state persisted for 75–91 ns depending on the solvent. The role of the rigid phenylacetylene bridge may be to slow down the charge-recombination process. The pyrazolino[60]fullerene, which is connected to dimethylaniline through an acetylene linkage, also plays a role giving rise to a radical ion pair with a longer lifetime.

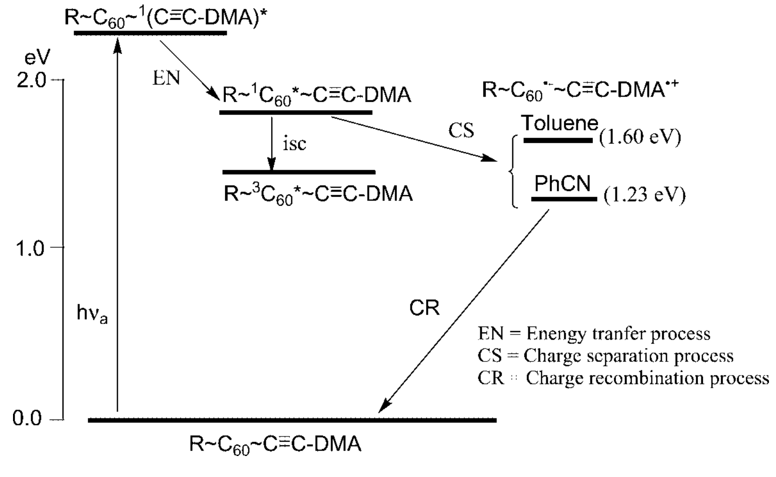

Figure 9. Energy diagram.

Experimental Section

Molecular Orbital Calculations: The computational calculations were performed by ab initio B3LYP/3-21G(*) methods using the GAUSSIAN03[23] software package on high speed computers. The images of the frontier orbitals were generated from Gauss View-03 software.

Instruments: The UV/Vis spectral measurements were carried out with a Jasco model V570 DS spectrophotometer. Steady-state fluorescence spectra were measured with a Shimadzu RF-5300 PC spectrofluorophotometer equipped with a photomultiplier tube having a high sensitivity in the 700–800 nm region. MALDI-TOF mass spectra were obtained with a VGAutoSpec spectrometer using ditranol as the matrix. Cyclic voltammetry measurements were obtained using a Versastat PAR EG & G potentiostat with analytical electrochemical software (Mod. 250). The measurements were taken in a double-walled cell (Metrohm EA 876–20). A glassy-carbon working electrode (Metrohm 6.0804.010) was used after being polished with alumina (0.3 μ) for 1 min and platinum wire was used as the counter electrode. An Ag/$AgNO_3$ electrode, used as a reference, was separated from the solution using a solution of tetrabutylammonium perchlorate, which was used as the supporting electrolyte, in benzonitrile. The samples were purged with argon prior to measurement.

The redox values were measured by differential pulse voltammetry (DPV) using a BAS CV-50W Voltammetric Analyzer (Japan). A platinum disk electrode was used as the working electrode, while a platinum wire served as a counterelectrode. An Ag/AgCl electrode was used as a reference. All measurements were carried out in different solvents containing 0.1 M tetrabutylammonium perchlorate $[(n\text{-Bu})_4NClO_4]$ as the supporting electrolyte. A scan rate of 0.1 V s^{-1} was used. Microwave irradiation was performed in a Discover® CEM instrument.

The picosecond time-resolved fluorescence spectra were measured by a single-photon counting method using the second harmonic generation (SHG, 400 nm) of a Ti:sapphire laser (Spectra-Physica, Tsunami 3950-L2S, 1.5 ps fwhm) and a streakscope (Hamamatsu Photonics) equipped with a polychromator (Action Research, SpectraPro 150) as an excitation source and detector, respectively. Lifetimes were evaluated using software attached to the equipment.

The nanosecond transient absorption spectra in the near-IR region were measured by laser flash photolysis; 355 nm light from a Nd:YAG laser (Spectra-Physics and Quanta-Ray GCR-130, 6 ns fwhm) was used as the excitation source. For transient absorption spectra in the visible (400–600 nm) and near-IR regions (600–1600 nm), monitoring lights from a pulsed Xe lamp were detected with Si- and Ge-avalanche photodiode modules, respectively. The samples were held in a quartz cell (1 × 1 cm) and were deaerated by bubbling argon gas through the solution for 15 min.

4-Nitrobenzaldehyde 4-Iodophenylhydrazone (2): A solution of 4-nitrobenzaldehyde (0.453 g, 3.0 mmol), 4-iodophenylhydrazine (1.05 g, 4.5 mmol) and two drops of acetic acid in ethanol (15 mL) was refluxed for 30 min. The solvent was evaporated in vacuo and the residual solid was purified by column chromatography (silica gel, hexane/ethyl acetate, 4:1) to give **2** as a red solid (0.825 g, 75%); m.p. 154–155 °C. FTIR (KBr): $\tilde{\nu}$ = 3283, 2926, 1591, 1561, 1514, 1479, 1334, 1262, 1157, 1104 cm^{-1}. ^{1}H NMR (200 MHz, $CDCl_3$): δ = 8.22 (d, J = 8.4 Hz, 2 H), 7.96 (s, 1 H), 7.76 (d, J = 8.4 Hz, 2 H), 7.69 (s, 1 H), 7.57 (d, J = 8.4 Hz, 2 H), 6.93 (d, J = 8.4 Hz, 2 H) ppm. ^{13}C NMR (50 MHz, $CDCl_3$): δ = 147.23, 143.32, 141.31, 138.13, 134.68, 126.39, 124.11, 115.18, 82.86 ppm.

4-Nitrobenzaldehyde 4-[4-(Dimethylamino)phenylethynyl]phenylhydrazone (4): $[(PPh_3)_2PdCl_2]$ (1 mg, 1.5 μmol) in piperidine (0.5 mL) was added to a stirred solution of **2** (184 mg, 0.5 mmol), 4-(dimethylamino)phenylacetylene (73 mg, 0.5 mmol), copper iodide (1 mg, 5.5 μmol) and triphenylphosphane (2.6 mg, 10 μmol) in freshly distilled piperidine (5 mL) under argon. The mixture was refluxed for 4 h. The reaction mixture was cooled and the solvent evaporated under vacuum. The crude product was purified by flash column chromatography (silica gel, hexane/dichloromethane, 1:2) to give **4** as a dark-red solid (140 mg, 73%); m.p. 169–171 °C. FTIR (KBr): $\tilde{\nu}$ = 3313, 2932, 2853, 2186, 1610, 1523, 1335, 1247, 1106, 816 cm^{-1}. ^{1}H NMR (200 MHz, $CDCl_3$): δ = 8.23 (d, J = 8.4 Hz, 2 H), 8.03 (s, 1 H), 7.78 (d, J = 8.4 Hz, 2 H), 7.71 (s, 1 H), 7.46 (d, J = 8.4 Hz, 2 H), 7.40 (d, J = 8.4 Hz, 2 H), 7.15 (d, J = 8.4 Hz, 2 H), 6.67 (d, J = 8.4 Hz, 2 H), 3.02 (s, 6 H) ppm. ^{13}C NMR (50 MHz, $CDCl_3$): δ = 149.87, 148.29, 146.84, 143.85, 142.06, 140.06, 136.18, 132.53, 127.76, 127.15, 123.93, 123.13, 114.51, 112.78, 111.86, 40.24 ppm.

General Procedure for the Cycloaddition Reactions: Pyridine (15 μL) was added to a solution of the appropriate hydrazone (0.14 mmol) in dry benzene (15 mL) under argon and the mixture was cooled to 0 °C. NCS (56 mg, 0.42 mmol) was added and the mixture was stirred for 10 min at this temperature and then warmed to room temperature (20 min). A solution of [60]fullerene (50 mg, 0.07 mmol) in dry toluene (50 mL) and triethylamine (1 mL) were added to the mixture and single-mode microwave irradiation (210 W) was applied for 50 min.

1′-(4-Iodophenyl)-3′-(4-nitrophenyl)pyrazolino[4′,5′:1,2][60]fullerene (3): Fullerene **3** was prepared following the general procedure described above. After flash column chromatography (silica gel, toluene) a yield of 26% (20 mg) was obtained. FTIR (KBr): $\tilde{\nu}$ = 2923, 1590, 1515, 1334, 1258, 1105, 945, 814 cm^{-1}. ^{1}H NMR (200 MHz, $CDCl_3$): δ = 8.56 (d, J = 8.4 Hz, 2 H), 8.36 (d, J = 8.4 Hz, 2 H), 7.78 (d, J = 2.8 Hz, 4 H) ppm. ^{13}C NMR (50 MHz, $CDCl_3$): δ = 147.61, 147.4, 147.16, 146.33, 146.24, 145.98, 145.88, 145.56, 145.43, 145.23, 145.13, 145.08, 144.60, 144.15, 143.81, 143.52, 143.13, 142.89, 142.84, 142.33, 142.09, 142.00, 141.82, 141.63, 140.32, 139.77, 138.52, 138.31, 136.51, 136.35, 128.92, 125.22, 123.99, 89.86, 80.72 ppm. UV/Vis (ODCB): $\lambda_{\max}$ (logε) = 429 (4.13), 330 (4.91), 298 (4.80) nm. MS (MALDI-TOF): m/z = 1084–1087 $[M]^+$.

1′-{4-[4-(Dimethylamino)phenylethynyl]phenyl}-3′-(4-nitrophenyl)pyrazolino[4′,5′:1,2][60]fullerene (1): Compound **1** was prepared in two different ways.

Route (a): Copper-free Sonogashira cross-coupling. Fullerene **3** (75 mg, 0.07 mmol), $[Pd(Ph_3)_4]$ (10% mol) and a large excess of piperidine (5 mL) were added to a solution of 4-(dimethylamino)phenylacetylene (10 mg, 0.07 mmol) in chlorobenzene (30 mL). The mixture was heated by single-mode microwave irradiation (300 W) in a sealed tube for 40 min. After solvent removal, the crude product was purified by flash column chromatography (silica gel, toluene) to yield 20% (15 mg) of fullerene **1**.

Route (b): Triad **1** was prepared following the general procedure described above and after flash column chromatography (silica gel, toluene) a yield of 30% (23 mg) was obtained. FTIR (KBr): $\tilde{\nu}$ = 2921, 1607, 1519, 1426, 1334, 1259, 1105, 943, 813, 753 cm^{-1}. ^{1}H NMR (200 MHz, $CDCl_3$): δ = 8.58 (d, J = 8.4 Hz, 2 H), 8.35 (d, J = 8.4 Hz, 2 H), 7.93 (d, J = 8.4 Hz, 2 H), 7.59 (d, J = 8.4 Hz, 2 H), 7.37 (d, J = 8.4 Hz, 2 H), 6.65 (d, J = 8.4 Hz, 2 H), 3.02 (s, 6 H) ppm. ^{13}C NMR (50 MHz, $CDCl_3$): δ = 147.31, 146.16, 146.08, 145.75, 145.44, 145.10, 145.02, 144.66, 144.02, 143.88, 142.98, 142.73, 142.18, 141.95, 141.67, 141.08, 140.64, 140.11, 139.61, 138.44, 137.27, 136.40, 136.15, 132.53, 132.05, 128.62, 123.74, 122.99, 121.31, 111.64, 110.02, 91.95, 87.26, 40.11 ppm. UV/Vis (ODCB): $\lambda_{\max}$ ($\log\varepsilon$) = 428 (4.10), 329 (4.89), 296 (4.81) nm. MS (MALDI-TOF): m/z = 1101–1104 $[M]^+$.

Acknowledgments

Financial support for this work was provided by the Ministerio de Educación y Ciencia of Spain and FEDER funds (Project CTQ2004-00364/BQU) and the Junta de Comunidades de Castilla-La Mancha (Project PAI-05-068). This work was also supported by a Grant-in-Aid for Scientific Research on Priority Area (417) from the Ministry of Education, Culture, Sports, Science, and Technology of the Japanese Government. M.E.E.-K. is grateful for a JSPS fellowship.

---

[1] L. Echegoyen, L. E. Echegoyen, *Acc. Chem. Res.* **1998**, *31*, 593–601.

[2] D. M. Guldi, M. Prato, *Acc. Chem. Res.* **2000**, *33*, 695–703.

[3] V. Balzani, *Electron Transfer in Chemistry*, vol. I–IV, Wiley-VCH, Weinheim, **2001**.

[4] a) H. Imahori, Y. Sakata, *Eur. J. Org. Chem.* **1999**, *10*, 2445–2457; b) D. M. Guldi, *Chem. Commun.* **2000**, *5*, 321–327.

[5] a) A. Gügel, J. Graus, J. Spickermann, P. Belik, K. Müllen, *Angew. Chem. Int. Ed. Engl.* **1994**, *33*, 559–561; b) R. M. Williams, J. M. Zwier, J. W. Verhoeven, *J. Am. Chem. Soc.* **1995**, *117*, 4093–4099; c) J. M. Lawson, A. M. Oliver, D. F. Rothenfluh, Y. Z. An, G. A. Ellis, M. G. Ranansinghe, S. I. Khan, A. G. Franz, P. S. Ganapathi, M. J. Shephard, M. N. Paddon-Row, Y. Rubin, *J. Org. Chem.* **1996**, *61*, 5032–5054; d) R. M. Williams, M. Koeberg, J. M. Lawson, Y. Z. An, Y. Rubin, M. N. Paddon-Row, J. W. Verhoeven, *J. Org. Chem.* **1996**, *61*, 5055–5062; e) S. G. Liu, L. Shu, J. Rivera, J. M. Raimundo, J. Roncali, A. Gorgues, L. Echegoyen, *J. Org. Chem.* **1999**, *64*, 4884–4886; f) D. M. Guldi, A. Swartz, C. Luo, R. Gómez, J. L. Segura, N. Martin, *J. Am. Chem. Soc.* **2002**, *124*, 10875–10886.

[6] P. J. Bracher, D. I. Schuster, *Electron Transfer in Functionalized Fullerenes* in *Fullerenes: From Synthesis to Optoelectronic Properties*, (Eds.: D. M. Guldi, N. Martín), Kluwer Academic Publishers, Dordrecht, **2002**, chapter 6.

[7] a) D. Gust, T. A. Moore, A. L. Moore, *Acc. Chem. Res.* **2001**, *34*, 40–48; b) D. M. Guldi, *Chem. Soc. Rev.* **2002**, *31*, 22–36.

[8] a) F. Langa, M. J. Gómez-Escalonilla, E. Diez-Barra, J. C. García-Martínez, A. de la Hoz, J. Rodríguez-López, A. González-Cortés, V. López-Arza, *Tetrahedron Lett.* **2001**, *42*, 3435–3438; b) F. Langa, P. de la Cruz, J. L. Delgado, M. J. Gómez-Escalonilla, A. González-Cortés, A. de la Hoz, V. López-Arza, *New J. Chem.* **2002**, *26*, 76–80; c) E. Espíldora, J. L. Delgado, P. de la Cruz, A. de la Hoz, V. López-Arza, F. Langa, *Tetrahedron* **2002**, *58*, 5821–5826.

[9] Y. Matsubara, H. Tada, S. Nagase, Z. Yoshida, *J. Org. Chem.* **1995**, *60*, 5372–5373.

[10] P. de la Cruz, A. Díaz-Ortiz, J. J. García, M. J. Gómez-Escalonilla, A. de la Hoz, F. Langa, *Tetrahedron Lett.* **1999**, *40*, 1587–1590.

[11] N. Armaroli, G. Accorsi, J. P. Gisselbrecht, M. Gross, V. Krasnikov, D. Tsamouras, G. Hadziioannou, M. J. Gomez-Escalonilla, F. Langa, J. F. Eckert, J. F. Nierengarten, *J. Mater. Chem.* **2002**, *12*, 2077–2087.

[12] a) C. Amatore, A. Jutand, *Acc. Chem. Res.* **2000**, *33*, 314–321; b) R. Rossi, A. Carpita, F. Bellina, *Org. Prep. Proced.***1995**, *27*, 127–160; c) K. Sonogashira, *Comprehensive Organic Synthesis* (Eds.: B. M. Trost, I. Fleming), Pergamon Press, Oxford, vol. 3, **1991**.

[13] N. E. Leadbeater, B. J. Tominack, *Tetrahedron Lett.* **2003**, *44*, 8653–8656.

[14] A. M. Ramos, M. T. Rispens, J. K. J. van Duren, J. C. Hummelen, R. A. J. Janssen, *J. Am. Chem. Soc.* **2001**, *123*, 6714–6715.

[15] K. A. Leonard, M. I. Nelen, L. T. Anderson, S. L. Gibson, R. Hilf, M. R. Detty, *J. Med. Chem.* **1999**, *42*, 3942–3952.

[16] a) F. Langa, P. de la Cruz, E. Espíldora, A. de la Hoz, J. L. Bourdelande, L. Sánchez, N. Martín, *J. Org. Chem.* **2001**, *66*, 5033–5041; b) J. J. Oviedo, P. de la Cruz, J. Garın, J. Orduna, F. Langa, *Tetrahedron Lett.* **2005**, *46*, 4781–4784.

[17] a) A. Weller, *Z. Phys. Chem., Neue Folge* **1982**, *133*, 93–98; b) D. Rehm, A. Weller, *Ber. Bunsen-Ges. Phys. Chem.* **1969**, *73*, 834–839.

[18] a) R. M. Noyes, *J. Am. Chem. Soc.* **1962**, *84*, 513–522; b) J. F. Coetzee, J. J. Camion, *J. Am. Chem. Soc.* **1967**, *89*, 2513–2517; c) S. Fukuzumi, J. K. Kochi, *J. Am. Chem. Soc.* **1982**, *104*, 7599–7609.

[19] a) P. A. Liddell, J. P. Sumida, A. N. Macpherson, L. Noss, G. R. Seely, K. N. Clark, A. L. Moore, T. A. Moore, D. Gust, *Photochem. Photobiol.* **1994**, *60*, 537–541; b) P. S. Baran, R. R. Monaco, A. U. Khan, D. I. Schuster, S. R. Wilson, *J. Am. Chem. Soc.* **1997**, *119*, 8363–8364; c) H. Imahori, M. E. El-Khouly, M. Fujitsuka, O. Ito, Y. Sakata, S. Fukuzumi, *J. Phys. Chem. A* **2001**, *105*, 325–332; d) H. Imahori, D. M. Guldi, K. Tamaki, Y. Yoshida, C. Luo, Y. Sakata, S. Fukuzumi, *J. Am. Chem. Soc.* **2001**, *123*, 6617–6628; e) F. D'Souza, G. R. Deviprasad, M. E. El-Khouly, M. Fujitsuka, O. Ito, *J. Am. Chem. Soc.* **2001**, *123*, 5277–5284; f) S. Fukuzumi, H. Imahori, H. Yamada, M. E. El-Khouly, M. Fujitsuka, O. Ito, *J. Am. Chem. Soc.* **2001**, *123*, 2571–2575; g) H. Imahori, Y. Mori, Y. Matano, *J. Photochem. Photobiol., C* **2003**, *4*, 51–83; h) M. E. El-Khouly, O. Ito, P. M. Smith, F. D'Souza, *J. Photochem. Photobiol., C* **2004**, *5*, 79–104.

[20] M. Fujutsuka, O. Ito, *Photochemistry of Fullerenes* in *Handbook of Photochemistry and Photobiology*, vol. 2, *Organic Photochemistry* (Ed.: H. S. Nalwa), American Science Publisher, CA, **2003**, vol. 2, pp. 111–145.

[21] a) R. A. Marcus, *J. Chem. Phys.* **1956**, *24*, 966–978; b) R. A. Marcus, *J. Chem. Phys.* **1957**, *26*, 867–871; c) R. A. Marcus, *J. Chem. Phys.* **1957**, *26*, 872–877; d) R. A. Marcus, *J. Chem. Phys.* **1965**, *43*, 679–701; e) R. A. Marcus, N. Sutin, *Biochim. Biophys. Acta* **1985**, *811*, 265–322.

[22] a) S. D. A. Sandanayaka, K. Matsukawa, T. Ishi-i, S. Mataka, Y. Araki, O. Ito, *J. Phys. Chem. B* **2004**, *108*, 19995–20004; b) H. Luo, M. Fujitsuka, Y. Araki, O. Ito, P. Padmawar, L. Chiang, *J. Phys. Chem. B* **2003**, *107*, 9312–9318.

[23] M. J. Frisch, G. W. Trucks, H. B. Schlegel, G. E. Scuseria, M. A. Robb, J. R. Cheeseman, J. A. Montgomery, Jr., T. Vreven, K. N. Kudin, J. C. Burant, J. M. Millam, S. S. Iyengar, J. Tomasi, V. Barone, B. Mennucci, M. Cossi, G. Scalmani, N. Rega, G. A. Petersson, H. Nakatsuji, M. Hada, M. Ehara, K. Toyota, R. Fukuda, J. Hasegawa, M. Ishida, T. Nakajima, Y. Honda, O. Kitao, H. Nakai, M. Klene, X. Li, J. E. Knox, H. P. Hratchian, J. B. Cross, V. Bakken, C. Adamo, J. Jaramillo, R. Gomperts, R. E. Stratmann, O. Yazyev, A. J. Austin, R. Cammi, C. Pomelli, J. W. Ochterski, P. Y. Ayala, K. Morokuma, G. A. Voth, P. Salvador, J. J. Dannenberg, V. G. Zakrzewski, S. Dapprich, A. D. Daniels, M. C. Strain, O. Farkas, D. K. Malick, A. D. Rabuck, K. Raghavachari, J. B. Foresman, J. V. Ortiz, Q. Cui, A. G. Baboul, S. Clifford, J. Cioslowski, B. B. Stefanov, G. Liu, A. Liashenko, P. Piskorz, I. Komaromi, R. L. Martin, D. J. Fox, T. Keith, M. A. Al-Laham, C. Y. Peng, A. Nanayakkara, M. Challacombe, P. M. W. Gill, B. Johnson, W. Chen, M. W. Wong, C. Gonzalez, J. A. Pople, *Gaussian 03*, revision C.02, Gaussian, Inc., Wallingford CT, USA, **2004**.

Received: November 17, 2005